

A Focused Library of Protein Tyrosine Phosphatase Inhibitors

Anthony B. Comeau,[†] David A. Critton,[‡] Rebecca Page,[‡] and Christopher T. Seto^{*,†}

[†]Department of Chemistry, Brown University, 324 Brook Street, Box H, Providence, Rhode Island 02912, and

[‡]Department of Molecular Biology, Cell Biology, and Biochemistry, Brown University, Box G-E4, Providence, Rhode Island 02912

Received April 30, 2010

Protein tyrosine phosphatases such as PTP1B and YopH are potential targets for the development of therapeutic agents against a variety of pathological conditions including diabetes, obesity, and infection by the bacterium *Yersinia pestis*. A focused library of bidentate α -ketoacid-based inhibitors has been screened against several tyrosine phosphatases. Compound **2a** has IC₅₀ values of 43 and 220 nM against YopH and PTP1B, respectively, and shows a 30-fold selectivity for PTP1B over the closely related phosphatase TCPTP.

Introduction

Intracellular signal transduction pathways are controlled by the reciprocal activities of protein kinases and phosphatases. Significant success has been achieved in the development of protein tyrosine kinase inhibitors. For example, the drugs imatinib and gefitinib are kinase inhibitors that are currently used to treat several cancers. In contrast, the development of drugs that target protein tyrosine phosphatases (PTPs^a) is less advanced.¹ The FDA has approved sodium stibogluconate, which is a potent inhibitor of the Src homology PTP 1 (SHP-1), SHP-2, and PTP1B,² as an orphan drug for cutaneous leishmaniasis. Isis Pharmaceuticals is developing an antisense drug that targets PTP1B for the treatment of type 2 diabetes,³ and a number of medicinal chemistry programs are underway to discover small molecule PTP inhibitors.¹ Two significant challenges to the development of orally bioavailable, small molecule inhibitors are: (1) many PTPs share similar structures and sequences in the region of their active sites, making it difficult to design inhibitors that are specific for their designated target, and (2) many small molecules that bind with high affinity in these active sites are hydrophilic, and as a result have poor cell permeability.¹

PTP1B was the first validated PTP target. It down regulates insulin signaling by dephosphorylating the insulin receptor and several of its downstream signaling proteins.⁴ PTP1B knockout mice show enhanced sensitivity to insulin and are resistant to diet induced weight gain, making this PTP an important target for both diabetes and obesity.⁵ T-Cell PTP (TCPTP) is highly homologous to PTP1B, with 74% sequence identity in the catalytic region. Unlike the PTP1B knockout mice that develop normally, the TCPTP knockout results in embryonic lethality caused by abnormalities in B- and T-cells.⁶ This observation suggests that it is desirable to achieve high

selectivity for PTP1B over TCPTP despite the similarity in the structures of their active sites.

A number of bacteria, including *Yersinia* and *Salmonella*, rely on PTPs for their pathogenicity.^{7,8} The *Yersinia pestis* bacterium, which causes bubonic plague, employs several virulence factors that it injects into the cytosol of eukaryotic cells using a contact-dependent type III secretion apparatus.⁹ One of these factors is the *Yersinia* PTP or YopH (*Yersinia* outer protein H). This PTP is essential for virulence of the bacterium; plasmids that lack a functional gene for this protein are not virulent.¹⁰ YopH compromises the host immune system by dephosphorylating host proteins including FAK (focal adhesion kinase), FYB (Fyn binding protein), the focal adhesion protein Cas, and SKAP-HOM (SKAP55 homologue).¹¹ In addition, YopH impairs T- and B-cell activation by inhibiting early phosphorylation reactions in the antigen receptor signaling complex.¹² Thus, YopH is a target for development of antibacterial agents against the bubonic plague.

HePTP is a phosphatase that is expressed in white blood cells in bone marrow, thymus, spleen, and lymph nodes. It represses T-cell activation and proliferation by binding to and dephosphorylating the activation loop of the MAP kinases Erk1, Erk2, and p38.¹³ HePTP is overexpressed in patients with the preleukemic disorder myelodysplastic syndrome and acute myelogenous leukemia, suggesting a link between abnormal HePTP activity and leukemia.¹⁴ Taken together, these observations reinforce the notion that PTPs are attractive targets for the development of small molecule inhibitors.

Table 1 shows a comparison of the sequences among four PTPs, PTP1B, TCPTP, HePTP, and YopH, in sections of the enzymes that are important for binding and catalysis. The P- and WPD-loops comprise the active site region of PTPs, while residues of the secondary site often interact with anionic functional groups on substrates and inhibitors. PTP1B and TCPTP are identical in these regions, while HePTP shows some variation from PTP1B in the secondary site and WPD-loop but not in the P-loop. YopH has differences from PTP1B in the WPD- and P-loops but has matching Arg residues in the secondary site.

We have been investigating aryl α -ketocarboxylic acids as nonhydrolyzable analogues of aryl phosphate esters.¹⁵

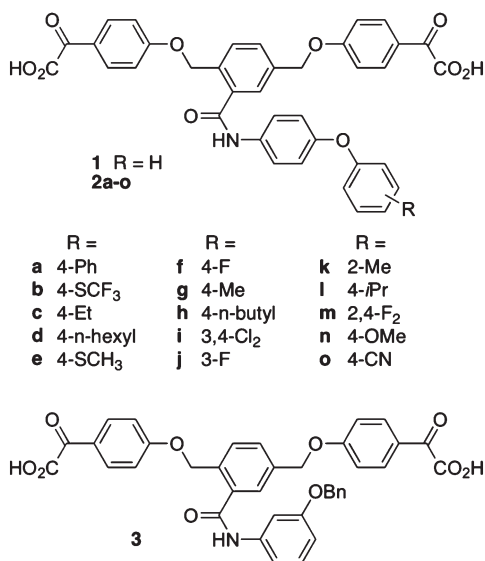
*To whom correspondence should be addressed. Phone: 401-863-3587. Fax: 401-863-9368. E-mail: christopher_seto@brown.edu.

^aAbbreviations: PTP1B, protein tyrosine phosphatase 1B; YopH, *Yersinia* outer protein H; TCPTP, T-cell protein tyrosine phosphatase; PTP, protein tyrosine phosphatase; SHP-1, Src homology protein tyrosine phosphatase 1; SHP-2, Src homology protein tyrosine phosphatase 2; HePTP, hematopoietic protein tyrosine phosphatase.

Table 1. Sequence Similarities among Four PTPs^a

PTP	secondary site	WPD-loop		P-loop	
		residues	sequence	residues	Sequence
PTP1B	R24, R254	179-185	WPDFGVP	214-221	HCSAGIGR
TCPTP	R25, R252	180-186	WPDFGVP	215-222	HCSAGIGR
HePTP	P 84, R306	234-240	WPD H QTP	269-276	HCSAGIGR
YopH	R205, R437	354-360	WPD Q TAV	402-409	G CRAGVGR

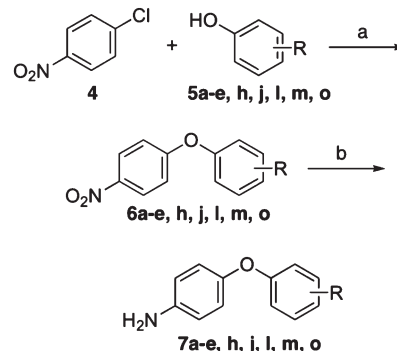
^a Sequence differences from PTP1B are highlighted in red.

**Figure 1.** Structures of inhibitors.

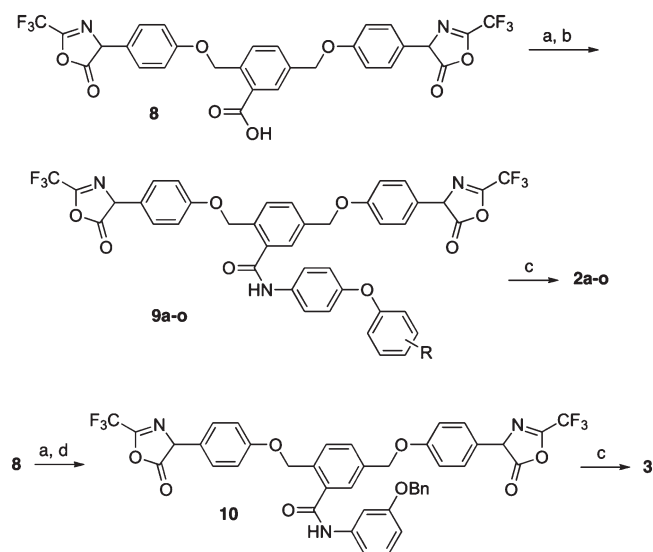
The α -ketocarboxylate is designed to have reduced negative charge at physiological pH when compared to phosphate esters and phosphonates and may give improved pharmacokinetic characteristics. However, this functional group retains enough anionic character to make strong interactions with the active and secondary sites of PTPs. In a recent study, we examined the activity of compound **1** (Figure 1),¹⁶ which incorporates two aryl α -ketoacid groups that are designed to contact both the active site and the secondary pTyr binding site.¹⁷ This inhibitor has IC₅₀ values of 240 nM and 1.5 μ M against YopH and PTP1B, respectively. However, it displays less than 2-fold selectivity for PTP1B over TCPTP. In an effort to improve the potency and specificity of **1**, we have constructed a focused library of inhibitors that incorporates substituents on the terminal diphenyl ether ring (**2a-o**). We have also examined compound **3**, which incorporates a 3-benzyloxy substituent. These compounds are optimized to interact with regions of PTPs outside of the catalytic site, including the secondary binding site.¹⁸ The inhibitors were screened in crude form using YopH, and four compounds were selected for purification and further analysis against YopH, PTP1B, TCPTP, and HePTP.

Chemistry

Before constructing the library, we needed to prepare the 4-phenoxyaniline analogues **7a-e, h, j, l, m, and o** (Scheme 1). These anilines were synthesized by S_NAr reaction of 4-chloronitrobenzene **4** with various phenols in the presence of potassium carbonate. The reactions were heated by microwave

Scheme 1. Synthesis of Anilines^a

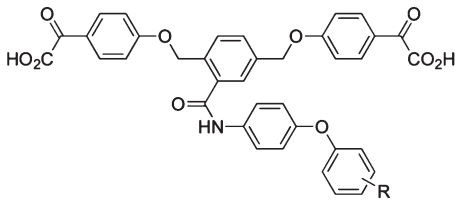
^a Reagents: (a) K₂CO₃, DMSO, microwave irradiation, 195 °C, 10 min; (b) 1 atm H₂, 10% Pd(OH)₂/C, EtOH. See Figure 1 for structures of the R groups.

Scheme 2. Synthesis of Inhibitors^a

^a Reagents: (a) SOCl₂, benzene; (b) CH₂Cl₂ or THF, anilines **7a-o**; (c) NaOH, H₂O; (d) 3-(benzyloxy)aniline. See Figure 1 and Scheme 1 for structures of the R groups. 3-(Benzyloxy)aniline and anilines **7f, g, i, k, and n** were obtained from commercial sources.

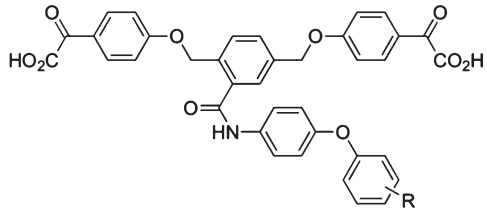
irradiation at 195 °C for 10 min. The resulting nitrobenzene derivatives **6** were reduced by catalytic hydrogenation using palladium hydroxide on carbon to give the desired anilines.

The inhibitors were synthesized as shown in Scheme 2. Compound **8**, which was prepared as reported previously,¹⁶ contains two trifluoromethyloxazolone groups. These trifluoromethyloxazolones, which are conveniently prepared by reaction of the corresponding 4-substituted phenylglycine derivative with trifluoroacetic anhydride,¹⁹ represent masked α -ketocarboxylic acids. The α -ketoacids can be unmasked at the end of the synthesis with aqueous base. The carboxylic acid group in **8** was converted to the acid chloride with thionyl chloride and subsequently reacted with anilines **7a-o** to give amides **9a-o**. The trifluoromethyloxazolones were then hydrolyzed with aqueous sodium hydroxide to give the crude inhibitors **2a-o**. In a similar manner, the acid chloride of **8** was reacted with 3-(benzyloxy)aniline to give **10**, which was hydrolyzed to generate inhibitor **3**. The purity of the crude inhibitors was determined to be $\geq 90\%$ by ¹H NMR spectroscopy.²⁰

Table 2. Inhibition of YopH by Crude Inhibitors **1**, **2a–o**, and **3**^a


compd	R	IC ₅₀ (nM)	compd	R	IC ₅₀ (nM)
2a	4-Ph	30	2i	3,4-Cl ₂	210
2b	4-SCF ₃	50	2j	3-F	220
2c	4-Et	70	2k	2-Me	230
2d	4- <i>n</i> -hexyl	90	1	H	240
3		100	2l	4- <i>i</i> Pr	800
2e	4-SCH ₃	110	2m	2,4-F ₂	910
2f	4-F	110	2n	4-OMe	1100
2g	4-Me	190	2o	4-CN	1300
2h	4- <i>n</i> -butyl	200			

^a Average of two measurements. The purity of the crude inhibitors was determined to be $\geq 90\%$ by ¹H NMR spectrometry. See Figure 1 for the structure of compound **3**.

Table 3. Inhibition of Phosphatases by Purified Inhibitors **2a–d**^a


compd	R	IC ₅₀ (μM)			
		YopH	PTP1B	TCPTP	HePTP
2a	4-Ph	0.043 ± 0.006	0.22 ± 0.04	6.5 ± 0.9	21 ± 5
2b	4-SCF ₃	0.063 ± 0.011	1.6 ± 0.2	4.0 ± 0.8	53 ± 4
2c	4-Et	0.053 ± 0.010	0.49 ± 0.07	3.5 ± 0.6	52 ± 8
2d	4- <i>n</i> -hexyl	0.089 ± 0.021	1.2 ± 0.2	2.3 ± 0.4	28 ± 3

^a Average of two measurements.

Enzyme Inhibition and Modeling Studies

The crude α -ketoacids were screened against YopH to gauge their potential as PTP inhibitors (Table 2). Many of the compounds show improved activity when compared to the parent inhibitor **1**. Only compounds that incorporated highly polar groups such as 2,4-F₂ (**2m**), 4-OMe (**2n**), and 4-CN (**2o**), or a bulky 4-*i*Pr substituent (**2l**), are weaker inhibitors than **1**. The most potent compounds with IC₅₀ values less than 100 nM incorporate hydrophobic substituents at the 4-position (compounds **2a–d**). It is unclear why inhibitor **2h**, which incorporates a 4-*n*-Bu substituent, is less active than the closely related inhibitors **2c** and **d**, which incorporate 4-Et and 4-*n*-hexyl substituents, respectively.

We purified the four most active compounds (**2a–d**) by HPLC and assayed them against four PTPs; YopH, PTP1B, TCPTP, and HePTP (Table 3). There is a good correlation between the IC₅₀ values obtained using crude and purified inhibitors, suggesting that the data obtained with the crude compounds provides a reliable indication of their true activity. In general, **2a–d** are potent YopH inhibitors with IC₅₀ values in the range of 43–89 nM. They also have reasonable activity against PTP1B, with values in the 0.22–1.6 μM range. Compound **2a** is the best inhibitor in the series against both

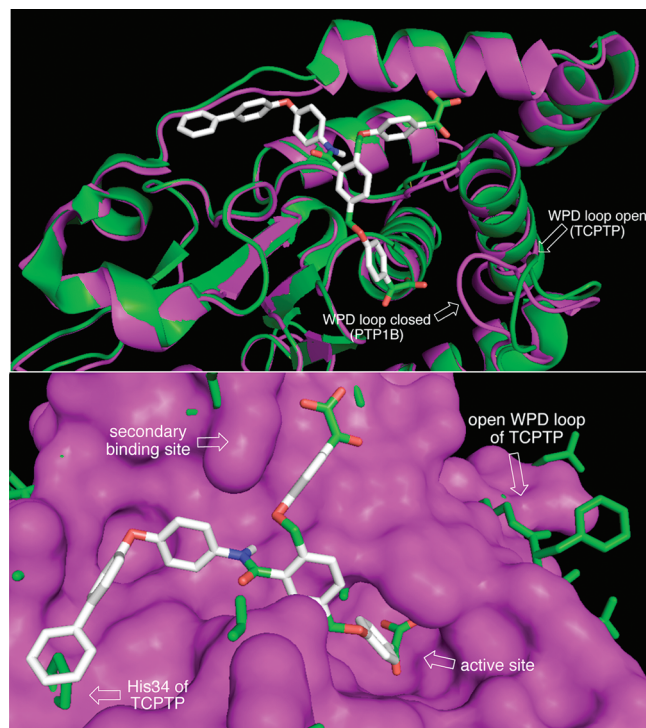


Figure 2. Model of inhibitor **2a** bound to PTP1B (pink). The structure of TCPTP (green) has been aligned with PTP1B. Top: Overlay of the ribbon diagrams of the two phosphatases. Bottom: The surface of PTP1B is superimposed on the stick diagram of TCPTP.

YopH and PTP1B. Importantly, it has a 30-fold selectivity for PTP1B over TCPTP. This is a significant level of selectivity given the high sequence homology shared by these two PTPs in their active site regions. By contrast, the parent inhibitor **1** has less than 2-fold preference for PTP1B over TCPTP.¹⁶ The added 4-phenyl substituent in **2a** when compared to **1** leads to improved selectivity by both increasing the compound's potency against PTP1B and decreasing potency against TCPTP. Compounds **2a–d** are modest inhibitors of TCPTP (IC₅₀ = 2.3–6.5 μM) and poor inhibitors of HePTP (IC₅₀ = 21–53 μM). Lineweaver–Burk analyses of compound **2b** against YopH, and compound **2a** against PTP1B, confirm that they are reversible competitive inhibitors.²⁰

We examined the potential binding mode of **2a** with PTP1B using molecular modeling. The X-ray structure of PTP1B bound to a difluorophosphonate inhibitor was used as the starting point (PDB code 1QXK).²¹ After the difluorophosphonate inhibitor was removed from the structure, **2a** was minimized in the active site using Autodoc Vina.²² The resulting model was aligned with the structure of TCPTP (PDB code 1L8K)²³ in an effort to identify features that may explain the selectivity of **2a** for PTP1B over TCPTP.

Figure 2 shows the model of **2a** minimized in the active site of PTP1B and superimposed on the structure of TCPTP. The top panel in Figure 2 highlights the high degree of similarity of these two phosphatases and emphasizes the difficulty in designing inhibitors that are selective for one enzyme over the other. One significant difference between the two structures is the position of the WPD loop. Only one crystal structure of TCPTP is available in the Protein Data Bank,²³ and this structure has the WPD loop in the open position. In contrast, the structure of PTP1B that we used for the minimization had the WPD loop closed onto a difluorophosphonate inhibitor.

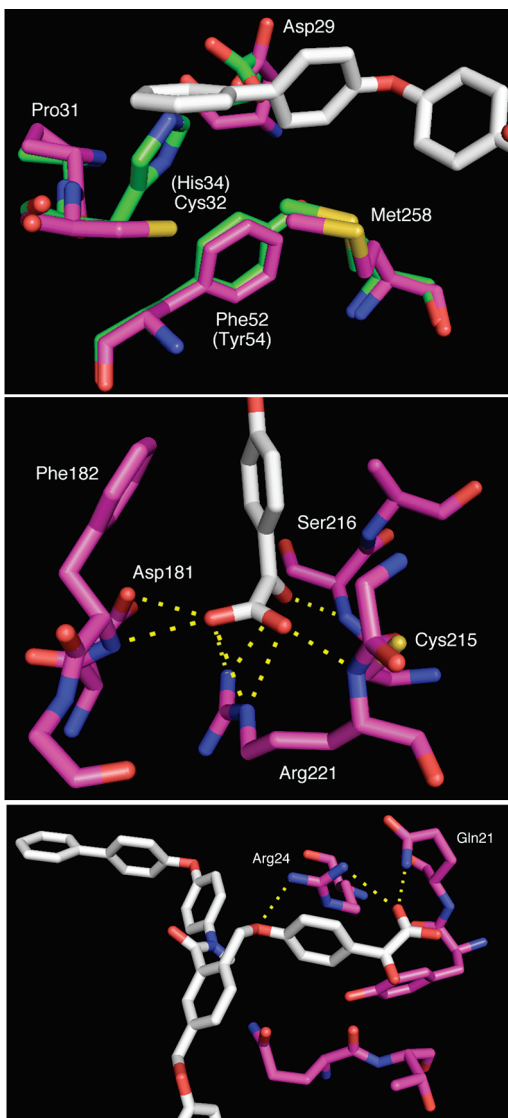


Figure 3. Interactions between inhibitor **2a** (white) and PTP1B (pink). Top: Model of the biphenyl portion of **2a** bound to PTP1B and superimposed on the crystal structure of TCPTP (green). Residues of TCPTP are listed in parentheses. Middle: Interactions between one α -ketocarboxylate of **2a** bound in the catalytic pocket of PTP1B. Bottom: Interactions between the second α -ketocarboxylate of **2a** and residues near the secondary binding site of PTP1B.

The bottom panel of Figure 2 highlights the differences between PTP1B and TCPTP that might be used to explain the selectivity of **2a** for PTP1B. One of the α -keto acid groups of **2a** binds deep in the active site pocket, similar to the binding of a natural pTyr substrate, and the second α -keto acid binds near Arg24 (PTP1B numbering) of the secondary site. One important difference between the two enzymes occurs in the region occupied by the terminal phenyl ring of the biphenyl subunit of **2a**. In PTP1B, the residue that is in closest proximity to this phenyl ring is Cys32. However, in TCPTP, the corresponding residue is His34, which is labeled in the bottom panel of Figure 2. The imidazole ring on the side chain of this residue can be seen emerging out of the pink surface of PTP1B directly underneath the terminal phenyl ring of **2a**.

Iversen and co-workers have identified six residues that are different between PTP1B and TCPTP that might be exploited for the design of specific inhibitors.²³ In the following list, PTP1B residues are outside of the parentheses, and the

corresponding TCPTP residues are inside parentheses. The six residues are Ala17 (Gln19), Gln21 (Leu23), Cys32 (His34), Lys39 (Glu41), Phe52 (Tyr54), and Ala264 (Pro262). As shown in detail in the top panel of Figure 3, our modeling results suggest that Cys32 (His34) may play an important role in determining the 30-fold selectivity of compound **2a** for PTP1B over TCPTP. The side chain of Cys32 of PTP1B resides below and parallel to the plane of the terminal phenyl ring of **2a**. In contrast, the side chain of His34 of TCPTP occupies the same region of space as the terminal phenyl ring in the **2a**/PTP1B model. Thus, a plausible explanation for the selectivity of **2a** for PTP1B over TCPTP is that His34 of TCPTP pushes the biphenyl subunit of **2a** into a different and presumably less favorable conformation in the binding site, which results in a lower overall binding energy between **2a** and TCPTP when compared with PTP1B. We note that the position of Cys32 in crystal structures of PTP1B with the WPD loop in the open (PDB code 2HNP)²⁴ and closed states²¹ are identical.

The middle panel in Figure 3 shows a more detailed view of the contacts between residues in the catalytic site of PTP1B and one of the α -ketocarboxylate groups of inhibitor **2a**. The carboxylate and ketone form a number of hydrogen bonds with backbone N–H atoms in both the P- and WPD-loops, including those of residues Phe182, Arg221, and Ser216. The inhibitor also forms hydrogen bonds with the side chains of Arg221 and Asp181. The benzene ring of the inhibitor forms a hydrophobic contact with the side chain of Phe182. The bottom panel of Figure 3 shows that the second α -keto acid can hydrogen bond with the side chains of Arg24 and Gln21 near the secondary site. The model also suggests a cation– π interaction between the neighboring phenyl ring of the inhibitor and the side chain of Arg24.

Conclusion

In summary, we have constructed a focused library of PTP inhibitors that are based upon the structure of compound **1**. Inhibitor **2a**, which incorporates a biphenyl substituent, emerged as the most potent compound in the library with IC₅₀ values of 43 and 220 nM against YopH and PTP1B, respectively. This inhibitor displays a significant level of selectivity for PTP1B over TCPTP. Molecular modeling studies indicate that the two α -ketocarboxylic acid groups in **2a** contact the catalytic and secondary sites and that the side chain of His34 of TCPTP may play an important role in the observed 30-fold selectivity of **2a** for PTP1B over TCPTP.

Experimental Section

General Methods. NMR spectra were recorded on Bruker Avance-300 or Avance-400 instruments. Spectra were calibrated using TMS ($\delta = 0.00$ ppm) for ¹H NMR, CDCl₃ ($\delta = 77.0$ ppm), acetone-*d*₆ ($\delta = 29.5$ ppm), or DMSO-*d*₆ for ¹³C NMR. Mass spectra were recorded using fast atom bombardment or electrospray ionization methods. Methylene chloride and methanol were obtained from a dry solvent dispensing system. HPLC analyses were performed on a Rainin HPLC system with C₁₈ columns and UV detection. All other reagents were used as received. The inhibitors **2a–d** were determined to be $\geq 95\%$ pure as measured by analytical reverse phase HPLC.

PTP Assays. The phosphatase activities of YopH, PTP1B, and TCPTP were assayed using *p*-NPP as the substrate at 25 °C, and the reaction progress was monitored using UV spectroscopy. Initial rates were determined by monitoring the hydrolysis of *p*-NPP at 420 nm, from 30 to 150 s after mixing. Percent inhibition assay solutions contained 10% DMSO, substrate

(*p*-NPP) was at the respective K_m for each PTP, 1 mM EDTA, 50 mM NaCl, and 50 mM 3,3-dimethylglutarate buffer at pH 7.0. The experimentally determined K_m values for *Yersinia* PTP, PTP1B, and TCPTP were 1.7, 2.3, and 1.7 mM, respectively. The activity of HePTP was assayed using 4-methylumbelliferyl phosphate (MUP) at 25 °C and the reaction progress was monitored using fluorescence spectroscopy. Initial rates were determined by monitoring the hydrolysis of MUP at excitation and emission wavelengths of 340 and 460 nm, respectively, from 0 to 150 s after mixing. Percent inhibition assay solutions for HePTP contained 10% DMSO, 174 μ M MUP, 1 mM EDTA, 50 mM NaCl, 50 mM 3,3-dimethylglutarate buffer at pH 7.0. The experimentally determined K_m value of MUP for HePTP was 174 μ M. IC_{50} values were calculated using the commercial graphing software Grafit (Erithacus Software Ltd.). Data were obtained for assays with at least five different concentrations, in duplicate, of each inhibitor.

Acknowledgment. This work was supported by an American Cancer Society Research Scholar Grant (RSG-08-067-01-LIB) to R.P.

Supporting Information Available: Synthetic procedures, compound characterization, HPLC traces for **2a–d**, Lineweaver–Burk analyses for compounds **2a** and **2b**. This material is available free of charge via the Internet at <http://pubs.acs.org>.

References

- (1) For recent reviews describing the development of small molecule PTP inhibitors, see: (a) Combs, A. P. Recent advances in the discovery of competitive protein tyrosine phosphatase 1B inhibitors for the treatment of diabetes, obesity, and cancer. *J. Med. Chem.* **2010**, *53*, 2333–2344. (b) Heneberg, P. Use of protein tyrosine phosphatase inhibitors as promising targeted therapeutic drugs. *Curr. Med. Chem.* **2009**, *16*, 706–733.
- (2) Pathak, M. K.; Yi, T. Sodium stibogluconate is a potent inhibitor of protein tyrosine phosphatases and augments cytokine responses in hemopoietic cell lines. *J. Immunol.* **2001**, *167*, 3391–3397.
- (3) Hardy, S.; Tremblay, M. L. Protein tyrosine phosphatases: new markers and targets in oncology? *Curr. Oncol.* **2008**, *15*, 5–8.
- (4) Kenner, K. A.; Anyanwu, E.; Olefsky, J. M.; Kusari, J. Protein tyrosine phosphatase 1B is a negative regulator of insulin- and insulin-like growth factor-I-stimulated signaling. *J. Biol. Chem.* **1996**, *271*, 19810–19816.
- (5) (a) Elchebly, M.; Payette, P.; Michaliszyn, E.; Cromlish, W.; Collins, S.; Loy, A. L.; Normandin, D.; Cheng, A.; Himms-Hagen, J.; Chan, C.-C.; Ramachandran, C.; Gresser, M. J.; Tremblay, M. L.; Kennedy, B. P. Increased insulin sensitivity and obesity resistance in mice lacking the protein tyrosine phosphatase-1B gene. *Science* **1999**, *283*, 1544–1548. (b) Klamann, L. D.; Boss, O.; Peroni, O. D.; Kim, J. K.; Martino, J. L.; Zabolotny, J. M.; Moghal, N.; Lubkin, M.; Kim, Y. B.; Sharpe, A. H.; Stricker-Krongrad, A.; Shulman, G. I.; Neel, B. G.; Kahn, B. B. Increased energy expenditure, decreased adiposity, and tissue-specific insulin sensitivity in protein-tyrosine phosphatase 1B-deficient mice. *Mol. Cell. Biol.* **2000**, *20*, 5479–5489.
- (6) You-Ten, K. E.; Muise, E. S.; Itie, A.; Michaliszyn, E.; Wagner, J.; Jothy, S.; Lapp, W. S.; Tremblay, M. L. Impaired bone marrow microenvironment and immune function in T cell protein tyrosine phosphatase-deficient mice. *J. Exp. Med.* **1997**, *186*, 683–693.
- (7) Bliska, J. B.; Guan, K. L.; Dixon, J. E.; Falkow, S. Tyrosine Phosphatase Hydrolysis of Host Proteins by an Essential *Yersinia* Virulence Determinant. *Proc. Natl. Acad. Sci. U.S.A.* **1991**, *88*, 1187–1191.
- (8) Kaniga, K.; Uralil, J.; Bliska, J. B.; Galan, J. E. A Secreted Protein Tyrosine Phosphatase with Modular Effector Domains in the Bacterial Pathogen *Salmonella typhimurium*. *Mol. Microbiol.* **1996**, *21*, 633–641.
- (9) Orth, K.; Palmer, L. E.; Bao, Z. Q.; Stewart, S.; Rudolph, A. E.; Bliska, J. B.; Dixon, J. E. Inhibition of the Mitogen-Activated Protein Kinase Kinase Superfamily by a *Yersinia* Effector. *Science* **1999**, *285*, 1920–1923.
- (10) Guan, K.; Dixon, J. E. Protein Tyrosine Phosphatase Activity of an Essential Virulence Determinant in *Yersinia*. *Science* **1990**, *249*, 553–556.
- (11) (a) Black, D. S.; Marie-Cardine, A.; Schraven, B.; Bliska, J. B. The *Yersinia* Tyrosine Phosphatase YopH Targets a Novel Adhesion-Regulated Signaling Complex in Macrophages. *Cell. Microbiol.* **2000**, *2*, 401–414. (b) Hamid, N.; Gustavsson, A.; Andersson, K.; McGee, K.; Persson, C.; Rudd, C. E.; Fallman, M. YopH Dephosphorylates Cas and Fyn-Binding Protein in Macrophages. *Microbial Pathog.* **1999**, *26*, 231–242.
- (12) Yao, T.; Mecsas, J.; Healy, J. I.; Falkow, S.; Chien, Y.-H. Suppression of T and B Lymphocyte Activation by a *Yersinia pseudotuberculosis* Virulence Factor, YopH. *J. Exp. Med.* **1999**, *190*, 1343–1350.
- (13) Mustelin, T.; Tautz, L.; Page, R. Structure of the Hematopoietic Tyrosine Phosphatase (HePTP) Catalytic Domain: Structure of a KIM Phosphatase with Phosphate Bound at the Active Site. *J. Mol. Biol.* **2005**, *354*, 150–163.
- (14) Zanke, B.; Squire, J.; Griesser, H.; Henry, M.; Suzuki, H.; Patterson, B. W. A Hematopoietic Protein Tyrosine Phosphatase (HePTP) Gene that is Amplified and Overexpressed in Myeloid Malignancies Maps to Chromosome 1q32.1. *Leukemia* **1994**, *8*, 236–244.
- (15) (a) Chen, Y. T.; Seto, C. T. Divalent and trivalent α -ketocarboxylic acids as inhibitors of protein tyrosine phosphatases. *J. Med. Chem.* **2002**, *45*, 3946–3952. (b) Xie, J.; Seto, C. T. A two stage click-based library of protein tyrosine phosphatase inhibitors. *Bioorg. Med. Chem. Lett.* **2007**, *15*, 458–474. (c) Xie, J.; Seto, C. T. Investigations of linker structure on the potency of a series of bidentate protein tyrosine phosphatase inhibitors. *Bioorg. Med. Chem.* **2005**, *13*, 2981–2991.
- (16) Chen, Y. T.; Seto, C. T. Parallel synthesis of a library of bidentate protein tyrosine phosphatase inhibitors based on the α -ketoacid motif. *Bioorg. Med. Chem.* **2004**, *12*, 3289–3298.
- (17) Puius, Y. A.; Zhao, Y.; Sullivan, M.; Lawrence, D. S.; Almo, S. C.; Zhang, Z.-Y. Identification of a second aryl phosphate-binding site in protein-tyrosine phosphatase 1B: a paradigm for inhibitor design. *Proc. Natl. Acad. Sci. U.S.A.* **1997**, *94*, 13420–13425.
- (18) Hu, X.; Vujanac, M.; Stebbins, C. E. Computational analysis of tyrosine phosphatase inhibitor selectivity for the virulence factors YopH and SptP. *J. Mol. Graphics Modell.* **2004**, *23*, 175–187.
- (19) Barnish, I. T.; Cross, P. E.; Danilewicz, J. C.; Dickinson, R. P.; Stepher, D. A. Promotion of carbohydrate oxidation in the heart by some phenylglyoxylic acids. *J. Med. Chem.* **1981**, *24*, 399–404.
- (20) See the Supporting Information.
- (21) Xin, Z.; Liu, G.; Abad-Zapatero, C.; Pei, Z.; Szczepankiewicz, B. G.; Li, X.; Zhang, T.; Hutchins, C. W.; Hajduk, P. J.; Ballaron, S. J.; Stashko, M. A.; Lubben, T. H.; Trevillyan, J. M.; Jirousek, M. R. Identification of a mono-based, cell permeable, selective inhibitor of protein tyrosine phosphatase 1B. *Bioorg. Med. Chem. Lett.* **2003**, *13*, 3947–3950.
- (22) Trott, O.; Olson, A. J. AutoDock Vina: improving the speed and accuracy of docking with a new scoring function, efficient optimization, and multithreading. *J. Comput. Chem.* **2010**, *31*, 455–461.
- (23) Iversen, L. F.; Moller, K. B.; Pedersen, A. K.; Peters, G. H.; Petersen, A. S.; Andersen, H. S.; Branner, S.; Mortensen, S. B.; Moller, N. P. H. Structure Determination of T cell protein-tyrosine phosphatase. *J. Biol. Chem.* **2002**, *277*, 19982–19990.
- (24) Barford, D.; Flint, A. J.; Tonks, N. K. Crystal Structure of Human Protein Tyrosine Phosphatase 1B. *Science* **1994**, *263*, 1397–1404.